

Wavelength-Dependent Photochemistry in Cr(CNPh)₆: A Study of Photosubstitution and Photoinduced Electron Transfer Using Time-Resolved Spectroscopy

Lawton E. Shaw and Cooper H. Langford*

Department of Chemistry, The University of Calgary, 2500 University Drive N.W.,
Calgary, Alberta T2N 1N4, Canada

Received March 10, 1999

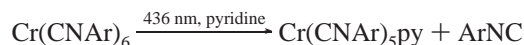
The wavelength dependence of photosubstitution, photoinduced electron transfer, and the time-resolved spectra of Cr(CNPh)₆, a compound having low-lying MLCT states, were investigated. Photosubstitution quantum yields increase with increasing excitation energy while photoinduced electron transfer quantum yields decrease with increasing excitation energy. At the lowest excitation energy used (532 nm, or 18 800 cm⁻¹), the quantum yields for both electron transfer and photosubstitution reach the same maximum value, 0.29. Picosecond time-resolved absorption spectra at 355 and 532 nm excitation wavelengths show two features: a bleach signal centered at 400 nm and an excited state absorption (ESA) in the 600 nm region. The ESA signal is much weaker for 532 nm excitations than for 355 nm excitations. Following a 355 nm flash, the bleach and ESA decay exponentially with the same lifetime of 23 μs. This implies a simple ligand dissociation followed by recombination. Bleach recovery kinetics after a 532 nm flash are more complicated: two or three exponential components are required to fit the data. Cr(CNPh)₆ exhibits two photochemical mechanisms: at high excitation energy, a simple charge neutral dissociation occurs; at low energy, it is proposed that a phenylisocyanide radical anion dissociates, forming a radical pair that is responsible for the observed substitution and electron transfer reactivity, and the complicated nanosecond kinetics. The primary processes for both reactions occur in less than 20 ps.

Introduction

Of recent interest in inorganic photochemistry is the problem of photosubstitution arising from the excitation of low-lying metal-to-ligand charge transfer (MLCT) states.^{1–5} MLCT states are commonly considered to be unreactive toward photosubstitution because they have little metal–ligand antibonding character.⁶ Substitutions from MLCT states might be expected to be associative in nature due to the increased positive charge at the metal center. It has become increasingly clear that substitutions arising from MLCT excitations can be very efficient and follow dissociative mechanisms. The most common model for this reactivity is population of higher lying ligand field (LF) states, from which ligand dissociation is known to occur.¹ Group 6 arylisocyanide complexes are interesting systems to study because of their low-lying MLCT states and the fact that antibonding ligand field (LF) states lie at much higher energies and are not expected to be directly populated at most irradiation wavelengths.^{7,8}

Photosubstitution and photoinduced electron transfer have been observed in chromium(0) hexakis(arylisocyanide) com-

plexes.⁹ In neat pyridine, Cr(CNAr)₆ undergoes photosubstitution:



The ligands phenylisocyanide (PhNC) and 2,6-diisopropylphenylisocyanide (CNIph) were used in order to compare the substitutional reactivity of Cr(CNAr)₆ complexes on the basis of steric effects.⁹ In both Cr(CNPh)₆ and Cr(CNIph)₆, the quantum yield for photosubstitution in pyridine was 0.23 (at 436 nm). This similarity in quantum yields for complexes with significantly different steric environments around the metal center led to the conclusion that the substitution proceeds via a dissociative mechanism. A more recent study of the wavelength dependence of the photosubstitution of Cr(CNPh)₆ in pyridine showed a decrease in ϕ_{sub} with increasing irradiation wavelength.⁴ This is typical of photodissociations where greater excitation energy corresponds to a greater probability of cage escape.

Only one time-resolved study has previously been reported on Cr(CNPh)₆, using THF as the solvent.¹⁰ It was proposed that the substitution product Cr(CNPh)₅(THF) accounted for the signal formed within a 1 ps pulse at 300 nm. Thus, ligand dissociation appears to occur in less than 1 ps. This places the photodissociation in the ultrafast regime observed for M(CO)₆ (M = Cr, Mo, W). An extremely weak emission from Cr(CNPh)₆ with $\tau < 10$ ns has been observed.⁷ The emission maximum is also subject to a significant Stokes shift. These

(1) Vichova, J.; Hartl, F.; Vlcek, A., Jr. *J. Am. Chem. Soc.* **1992**, *114*, 10903.

(2) Rossenaar, B. D.; Kleverlaan, C. J.; Stufkens, D. J.; Oskam, A. *J. Chem. Soc., Chem. Commun.* **1994**, 63.

(3) Stufkens, D. J.; van Outersterp, J. W. M.; Oskam, A.; Rossenaar, B. D.; Stor, G. J. *Coord. Chem. Rev.* **1994**, *132*, 147.

(4) Maskova, E.; Vlcek, A., Jr. *Inorg. Chim. Acta* **1996**, *242*, 17.

(5) Lindsay, E.; Vlcek, A., Jr.; Langford, C. H. *Inorg. Chem.* **1993**, *32*, 2269.

(6) Geoffroy, G. L.; Wrighton, M. S. *Organometallic Photochemistry*; Academic Press: New York, 1979.

(7) Mann, K. R. Ph.D. Thesis, California Institute of Technology, 1977.

(8) Mann, K. R.; Cimolino, M.; Geoffroy, G. L.; Hammond, G. S.; Orio, A. A.; Albertin, G.; Gray, H. B. *Inorg. Chim. Acta* **1976**, *16*, 97.

(9) Mann, K. R.; Gray, H. B.; Hammond, G. S. *J. Am. Chem. Soc.* **1977**, *99*, 306.

(10) Xie, X.; Simon, J. D. *J. Phys. Chem.* **1989**, *93*, 4401.

observations are suggestive of weakly bound excited states (i.e., the system does not thermally relax into a well-defined potential well from which emission can occur). This agrees with the ultrafast nature of the ligand dissociation.

Photoinduced electron transfer has also been observed for $\text{Cr}(\text{CNAr})_6$ complexes in chlorocarbon solvents.^{7,9} The first model for this electron transfer reactivity is based on electron transfer directly from the MLCT excited state. In $\text{Cr}(\text{CNIph})_6$, irradiation at 436 nm in degassed chloroform gives the one electron oxidation product $\text{Cr}(\text{CNIph})_6^+$ with a quantum yield of 0.19. The quantum yield rises to 0.70 in air-saturated chloroform. The interpretation is that oxygen acts to scavenge the electron transfer products (i.e., radicals) that are formed from excited state electron transfer to the electron acceptor solvent. In $\text{Cr}(\text{CNPh})_6$, a $\text{Cr}(\text{II})$ product is formed on irradiation in chloroform.

Photochemical ligand substitution and electron transfer reactions are not unusual for metal complexes with MLCT states, but these chromium isocyanide complexes are unique in that both substitution and bimolecular electron transfer are known to occur in systems where there are no long-lived excited states. Here we present a complete study of the wavelength-dependent photochemistry in $\text{Cr}(\text{CNPh})_6$ and propose a new model for the excited state reactivity that reconciles the known ultrafast nature of the primary photochemical steps to the kinetic requirements of bimolecular electron transfer.

Experimental Section

General Procedures. All irradiations were performed under nitrogen using standard Schlenk techniques. Benzene was distilled from sodium benzophenone ketyl, and pyridine was distilled from calcium hydride. Benzoquinone was recrystallized from hexane prior to use.

Materials. Phenylisocyanide was prepared from aniline, sodium hydroxide, and chloroform according to the method of Ugi et al.¹¹ Chromium(0) hexakisphenylisocyanide was obtained from chromous acetate and phenylisocyanide using the method of Mann.⁸ Elemental anal. Calcd: C, 75.20; H, 4.52; N, 12.53. Found: C, 75.04; H, 4.57; N, 12.86.

Steady State Quantum Yield Measurements. Steady state reactions were monitored by UV-visible spectroscopy. Molar absorptivities of reactants were determined by measuring the absorbance of solutions with an accurately weighed quantity of the appropriate compound. Molar absorptivities of products were determined by irradiating samples with known concentrations of reactant to 100% conversion and measuring the absorbance. Molar absorptivities measured this way have uncertainties in the range 5–10%. Absorption spectra for molar absorptivities and quantum yield measurements were recorded using a Hewlett-Packard model 8452A diode array spectrophotometer interfaced to a PC computer. Resolution of the instrument is ± 2 nm.

All samples were prepared in the dark with a red safety light. Due to the air sensitivity of many of the solutions, all samples were subject to three to five freeze/pump/thaw cycles (in the cell) under nitrogen to remove traces of oxygen. Solvents and solutions were transferred under nitrogen using transfer needles or syringes. Glassware was cleaned and then dried in a 110 °C oven for 1 h before use. The concentration of $\text{Cr}(\text{CNPh})_6$ was chosen such that samples absorbed >99% of light at the irradiation wavelength. $\text{Cr}(\text{CNPh})_6$ concentrations were between 4×10^{-5} and 5×10^{-4} M. The cell used for the irradiation of samples was equipped with a fused quartz-glass joint to a Teflon stopcock and sidearm with bulb for freeze/pump/thaw cycles. A separate matched cell was used for ferrioxalate and reineckate actinometry. Samples and actinometer solutions were stirred continuously during irradiations with a magnetic stir bar (9 mm long, 2 mm in diameter) rotating perpendicular to the incident light.

The light source for 313, 365, 436, and 532 nm was a PRA model ALH 215 xenon medium-pressure arc lamp (150 W) coupled with the appropriate interference filter. For 514.0 nm, a Spectra-Physics model 164 argon ion laser was used. The light sources were attenuated with

Table 1. $\text{Cr}(\text{CNPh})_6$ Substitution Quantum Yields in Benzene

wavelength (nm)	quantum yield ^a	
	0.1 M pyridine	0.1 M PPh_3
313	0.54	
365	0.42	0.42
436	0.38	0.39
514	0.29	0.28
532	0.28	

^a All quantum yields have standard deviations of ± 0.01 .

neutral density filters to obtain intensities appropriate for measurements of small, accurate absorption changes over time intervals of 15–60 s. Light intensities at 313, 365, and 436 nm were determined using the potassium ferrioxalate.¹² Light intensities at 514 and 532 nm were determined by either reineckate actinometry¹³ or fulgide actinometry.¹⁴ Reineckate and fulgide actinometers were calibrated to the ferrioxalate actinometer at 436 nm. The calculation of moles of product formed was obtained by monitoring the decrease of reactant absorption (electron transfer reactions) or by increase of product absorption (all substitution reactions).

Nanosecond Flash Photolysis. The nanosecond flash photolysis experiments were performed using the system at the chemistry department at the University of Victoria. This system has been described in detail elsewhere.¹⁵ Time resolution is 20 ns.

Picosecond Absorption Spectroscopy. Picosecond time-resolved studies were performed at the Canadian Centre for Picosecond Laser Spectroscopy, Montreal, Quebec. The system is described in detail elsewhere.¹⁶ The system is based on a mode-locked Nd:YAG laser that is frequency doubled to give second and third harmonic frequencies (532 and 355 nm) for the pump pulse. The continuum probe pulse is generated by passing part of the pump pulse through a solution of D_3PO_4 . An optical delay line generates the time delay between pump and probe pulses. Final pump and probe pulses have a width of 35 ps at half-maximum intensity, allowing for 17 ps time resolution at 0 ps time delay. Pump pulse energies were between 1 and 2.5 mJ, which is expected to excite 100% of the absorbing molecules. Spectra did not change noticeably with variations in pump energy, implying that secondary photolysis was not important.

Results

Photosubstitution. To confirm the dissociative mechanism of photosubstitution in $\text{Cr}(\text{CNPh})_6$, the dependence of ϕ_{sub} on nucleophile was studied. Quantum yields were determined in benzene containing a low concentration of nucleophile. This avoids the complications of solvent effects, which can account for large variations in substitution quantum yields. The nucleophiles pyridine and triphenylphosphine (PPh_3) were used. Table 1 gives the quantum yields for photosubstitution in benzene containing 0.1 M of nucleophile, at various wavelengths. Within experimental error, there is no difference in ϕ_{sub} with pyridine or PPh_3 . The insensitivity to entering group indicates a dissociative or solvent-mediated mechanism. No evidence for attack by strong nucleophiles emerged.

In benzene and neat pyridine, the quantum yields decrease with increasing irradiation wavelength (Figure 1). This is a typical pattern in photodissociation reactions of metal complexes, where greater excess excitation energy translates into more efficient cage escape. The differences in quantum yield

- Weber, W. P.; Gokel, G. W.; Ugi, I. K. *Angew. Chem., Int. Ed. Engl.* **1972**, *11*, 530.
- Hatchard, C. G.; Parker, C. A. *Proc. R. Soc. London* **1956**, A235, 518.
- Wegner, E. E.; Adamson, A. W. *J. Am. Chem. Soc.* **1966**, *88*, 394.
- Heller, H. G.; Langan, J. R. *J. Chem. Soc., Perkin Trans. 2* **1981**, 341.
- Liao, Y.; Bohne, C. *J. Phys. Chem.* **1996**, *100*, 734.
- Moralejo, C.; Langford, C. H.; Sharma, D. K. *Inorg. Chem.* **1989**, *28*, 2205.

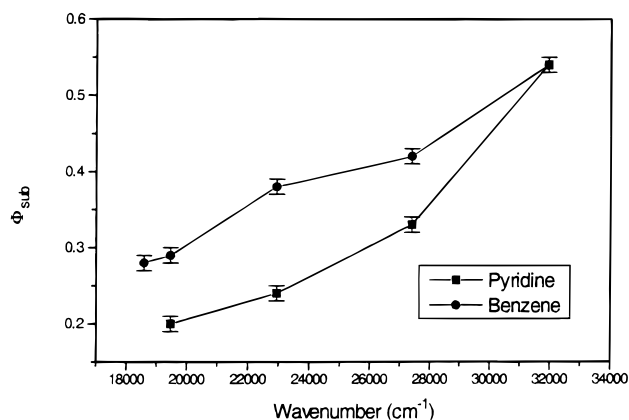


Figure 1. Excitation energy dependence of photosubstitution quantum yields ϕ_{sub} for $\text{Cr}(\text{CNPh})_6$ in pyridine (■) and 0.1 M pyridine in benzene (●). Error bars represent the standard deviation for each data point.

between these two solvents are relatively small and are attributed to solvent effects. The overall trends in ϕ_{sub} with wavelength are similar.

Electron Transfer. The previous study on photoinduced electron transfer in $\text{Cr}(\text{CNPh})_6$ used the solvent chloroform as the electron acceptor.^{7,9} In that study it was assumed that the initial electron transfer occurred directly from the MLCT excited state. The chlorinated solvent acted as an efficient electron acceptor. This experiment did not allow for any estimate of the lifetime of the reactive state. Since the electron acceptor was always in a state of encounter with the complex, it is impossible to estimate the lifetime of the reactive state using the acceptor concentration and the rate of diffusion in that solvent.

To avoid the possible complications that may arise due to Cl radical formation and to estimate the lifetime of the reactive state, it was chosen to study the electron transfer using a moderate concentration of an organic electron acceptor in an inert organic solvent. A stable reduced organic acceptor avoids the potential problems arising from Cl radical attack on the metal center. The second advantage is that the dependence of electron transfer efficiency on acceptor concentration can yield a crude estimate of the lifetime of the reactive species. The acceptor benzoquinone (BQ) was chosen because it has a reduction potential (-0.585 V vs Ag/AgCl)¹⁷ similar to the potential for the Cr^+/Cr^0 couple in $\text{Cr}(\text{CNPh})_6$ (-0.53 V in CH_3CN vs Ag/AgCl).¹⁸ Because of the similar E° 's, thermal electron transfer in the ground state and back electron transfer among the photoproducts are hindered due to overpotential. Indeed, the rate of ground state electron transfer between $\text{Cr}(\text{CNPh})_6$ and BQ was too slow to be detected over several hours.

When $\text{Cr}(\text{CNPh})_6$ is irradiated in benzene in the presence of BQ, precipitates are formed. This is evidence for an electron transfer reaction that forms ionic products which are insoluble in the nonpolar solvent. The product(s) are likely $\{\text{Cr}^{\text{II}}\text{L}_6^{2+}, \text{BQ}^{\cdot-}\}$ or $\{\text{Cr}^{\text{III}}\text{L}_6^{3+}, \text{BQ}^{\cdot-}\}$ salts, where L is either PhNC or BQ. To hinder precipitate formation, a solvent mixture of phenylisocyanide/benzene (10 vol %) was used. By using phenylisocyanide as the cosolvent, substitution processes do not complicate the data analysis. An EPR spectrum taken after irradiation of $\text{Cr}(\text{CNPh})_6$ and BQ in PhNC/benzene revealed a complex signal consisting of about 13 equally spaced peaks in a complex intensity ratio (see Supporting Information). While

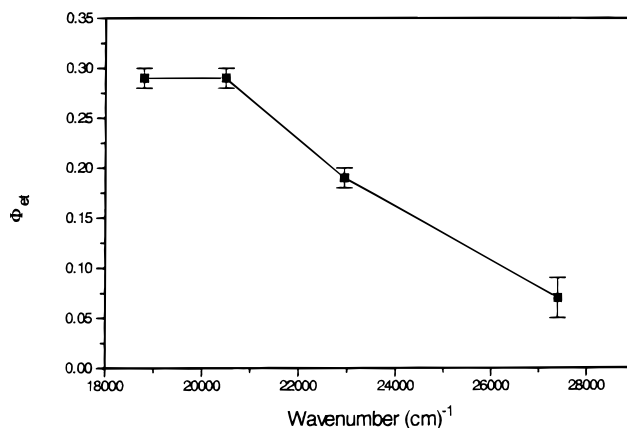


Figure 2. Excitation energy dependence of quantum yields of photoinduced electron transfer between $\text{Cr}(\text{CNPh})_6$ and benzoquinone. Error bars represent the standard deviation for each data point. The quantum yield at 313 nm was not measured because of the large BQ absorption at this wavelength, which interferes significantly with light absorption by $\text{Cr}(\text{CNPh})_6$. BQ absorption at other wavelengths was accounted for in the quantum yields shown here.

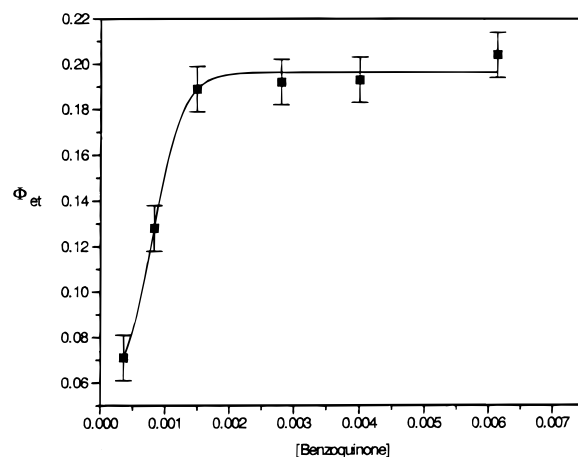


Figure 3. Quantum yields for decomposition of $\text{Cr}(\text{CNPh})_6$ in 10% phenylisocyanide/benzene at 436 nm with varying benzoquinone concentrations. Error bars represent standard deviation.

the EPR spectrum of the benzoquinone radical anion is not salient, this is not surprising since the radical is expected to be intimately associated with the charged chromium complex in this nonpolar medium. Such an association could perturb and complicate the signal dramatically. The signal is stable indefinitely and provides proof of an irreversible photochemical electron transfer reaction.

Electron transfer quantum yields (ϕ_{et}) were obtained by monitoring the loss in $\text{Cr}(\text{CNPh})_6$ absorption. The wavelength dependence for the photoinduced electron transfer reaction between $\text{Cr}(\text{CNPh})_6$ and BQ is shown in Figure 2. The quantum yield increases from 0.07 at 365 nm to a limit of 0.29 between 514 and 532 nm (identical to ϕ_{sub} at these wavelengths). The wavelength dependence of electron transfer is significantly different from the dependence for substitution. The interpretation of a quantum yield that *increases with decreasing excitation energy* is that there is a low-energy state that is responsible for the electron transfer reaction, and that excitation at higher energies does not lead to efficient population of this state. Such a wavelength dependence cannot be explained by a simple model using only thermally equilibrated excited states.

Figure 3 shows the variation of ϕ_{et} with BQ concentration under 436 nm irradiation. It can be seen that the maximum limit

(17) Bard, A. J.; Faulkner, L. R. *Electrochemical Methods: Fundamentals and Applications*; John Wiley and Sons: New York, 1980.

(18) Bohling, D. A.; Evans, J. F.; Mann, K. R. *Inorg. Chem.* **1982**, *21*, 3546.

of ϕ_{et} is reached at BQ concentrations of 2–3 mM. In benzene, the diffusion-controlled rate constant, k_{diff} , can be estimated by the Smoluchowski–Stokes–Einstein equation. For reactions at 20 °C in benzene, k_{diff} is estimated at $\leq 1.0 \times 10^{10} \text{ M}^{-1} \text{ s}^{-1}$.¹⁹ Because ϕ_{et} remains limiting at 2 mM, the species responsible for electron transfer must have a lifetime in excess of $\tau = [(2 \times 10^{-3} \text{ M})(1.0 \times 10^{10} \text{ M}^{-1} \text{ s}^{-1})]^{-1} = 50 \text{ ns}$ since the maximum rate constant is k_{diff} . This lifetime cannot correspond to an excited state since it is known that the excited state decays on the ultrafast time scale. An excited state electron transfer is therefore unlikely under these conditions.

Time-Resolved Spectroscopy. The photochemistry of Cr(CNPh)₆ was examined using nanosecond flash photolysis. Cr(CNPh)₆ is relatively nonreactive in neat benzene, although there is a small degree of permanent bleaching ($\phi \approx 0.05$ at 436 nm). This makes benzene an appropriate medium in which to monitor the fate of transients. Cr(CNPh)₆ in benzene was excited with both 355 and 532 nm flashes. There are two absorption features observed in the time-resolved spectra of Cr(CNPh)₆: (1) bleach signal; (2) excited state absorption (ESA). Here, an ESA is operationally defined as an absorption with a greater intensity than the ground state absorption at that wavelength. Either an excited state or initial photoproducts can be responsible for an ESA. The kinetics of bleach recovery (monitored at 400 nm) and ESA decay (monitored at 630 nm) were measured.

For 355 nm flashes, both the bleach recovery and ESA decay are simple monoexponentials, each having a lifetime of $\tau = 23 \mu\text{s}$. These single-exponential fits must correspond to the “pseudo” first-order reaction²⁰



The ESA signal observed in the long-wavelength region (630 nm) is therefore assigned to Cr(CNPh)₅S. Solvent molecules coordinated to vacant coordination sites are well-known species.²¹ Many “nonreactive” aliphatic and aromatic solvents are known to coordinate to the vacant coordination sites created by the photodissociation of an original ligand. The resulting “solvo” complexes, often referred to as σ -complexes, are inherently labile and typically react with incoming ligands near diffusion-limited rates.

For 532 nm flashes, the Cr(CNPh)₅S signal at 630 nm also decays as a single exponential, and with an apparent lifetime of $\tau = 23 \mu\text{s}$. However, the signal is very weak and therefore the lifetime is subject to a degree of uncertainty due to increased relative noise (see Supporting Information).

The bleach recovery for 532 nm excitation is not a simple exponential, and a fit required two or more exponentials. Knowing that there should be a 23 μs component, the data were fitted with two additional unknown exponentials. These other components were found to have lifetimes of 12 and 214 μs . This fit suggests two other reactions at 532 nm that occur in

(19) Murov, S. L.; Carmichael, I.; Hug, G. L. *Handbook of Photochemistry*, 2nd ed.; Marcel Dekker: New York, 1993.

(20) The kinetics observed are indistinguishable from first order and therefore must involve a species such as {Cr(CNPh)₅⋯PhNC} or {Cr(CNPh)₅S⋯PhNC}. The assignment of the ESA to a solvo species does not exclude the possibility of weak coordination of the PhNC ligand to the chromium center via the phenyl group, an isomer which would be spectroscopically similar to a true solvo species in this solvent (benzene). The 23 μs lifetime is too long a time scale for the survival of an encounter complex without ionic or bonding interactions.

(21) (a) Jones, W. D.; Feher, F. J. *J. Am. Chem. Soc.* **1984**, *106*, 1650. (b) Hoyano, J. K.; Graham, W. A. G. *J. Am. Chem. Soc.* **1982**, *104*, 3723. (c) Janowicz, A. H.; Bergman, R. G. *J. Am. Chem. Soc.* **1983**, *105*, 3929.

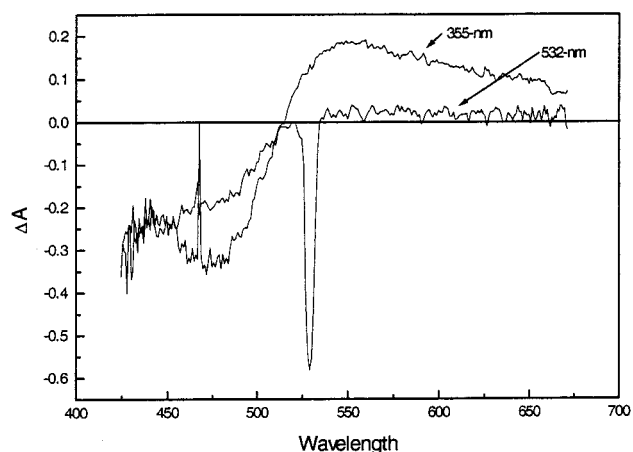


Figure 4. Transient absorption spectra at 20 ps time delay using 355 and 532 nm excitation wavelengths. Standard deviation of the signal is up to ± 0.05 absorbance units.

addition to the charge neutral back reaction responsible for the 355 nm kinetics. Apparently, these other reactions are independent of the decay of the 630 nm signal, already assigned to Cr(CNPh)₅S. These reactions will be discussed below.

Picosecond absorption spectra of Cr(CNPh)₆ in neat benzene for 355 and 532 nm excitation are shown for the 20 ps time delay in Figure 4. The 20 ps spectrum for 355 nm excitation shows a large bleach signal (at approximately 420–520 nm) and a large ESA in the long-wavelength region (520–640 nm). This ESA was assigned to the solvated species Cr(CNPh)₅S above. The long wavelength Cr(CNPh)₅S signal is fully formed within the 355 nm pulse (i.e., <20 ps). The 20 ps spectrum for 532 nm excitation is noticeably different. The bleach signal remains, but the Cr(CNPh)₅S absorption is significantly weaker than under 355 nm excitation.

For instrumental reasons, these spectra provide measurements in true absorbance units, unlike the nanosecond data above. This allows for quantitative comparisons between spectra, provided that ground state absorbances (or concentrations) are known. At the laser intensities used here, 100% of all absorbing molecules exposed to the laser flash are excited, thus simplifying the comparisons. The relative efficiencies for Cr(CNPh)₅S formation between 355 and 532 nm can be calculated according to

$$\frac{\phi_{355}}{\phi_{532}} = \frac{\left(\frac{\Delta A_{600,355}}{[\text{Cr(CNPh)}_6]_{355}} \right)}{\left(\frac{\Delta A_{600,532}}{[\text{Cr(CNPh)}_6]_{532}} \right)}$$

The change in absorbance ΔA_{600} was used because the ground state absorbance is negligible at this wavelength and there should be no bleach overlap. The concentrations of Cr(CNPh)₆ were determined from UV–vis absorption. All other terms cancel out and are not shown in the equation. Using this equation and the data in Figure 4, $\phi_{355}/\phi_{532} \approx 20$. The relative efficiency of Cr(CNPh)₅S formation is at least 20 times greater at 355 nm than at 532 nm.

Discussion

Resonance Raman experiments have shown the presence of a unique band in the long-wavelength region.⁴ Between 454.5 and 514.5 nm, the signals for the $\delta(\text{Cr}–\text{C}–\text{N})$ and $\delta(\text{C}–\text{Cr}–\text{C})$ bending modes dramatically increase in intensity. The excited

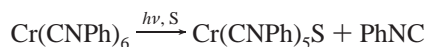
state displacements along two normal coordinates (Δ_a , Δ_b) can be compared according to

$$\frac{I_a}{I_b} = \frac{\omega_a^2 \Delta_a^2}{\omega_b^2 \Delta_b^2}$$

where I_a and I_b are the intensities of the bands in the preresonance Raman spectrum and ω_a and ω_b are the frequencies. Relative to the $\nu(\text{C}\equiv\text{N})$ mode, the *relative* displacements of the $\delta(\text{Cr}-\text{C}-\text{N})$ and $\delta(\text{C}-\text{Cr}-\text{C})$ modes increase from 2.7 to 7.2 and 0 to 11.7, respectively, on going from 454.5 to 514.5 nm. There is clearly a unique absorption in the tail of the broad MLCT absorption that is responsible for these large excited state distortions.

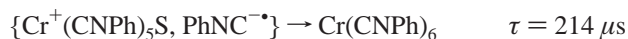
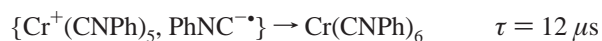
The wavelength dependence of electron transfer above (Figure 2) confirms the presence of a unique absorption in the low-energy region of the MLCT envelope. This wavelength dependence not only identifies a reactive low-energy excited state but distinguishes it from higher energy excited states: the wavelength dependence of photosubstitution (Figure 1) clearly shows that labile excited states are present in a region of the absorption spectrum where the electron transfer reactivity falls off. Thus, there are two distinct photochemical behaviors, and we propose the following two pathways:

1. Charge Neutral Photosubstitution.



This involves the heterolytic dissociation of a neutral PhNC ligand. This pathway is proposed to be responsible for the simple monoexponential 23 μs recoveries in the nanosecond data for 355 nm excitation. This pathway is dominant in the UV wavelengths.

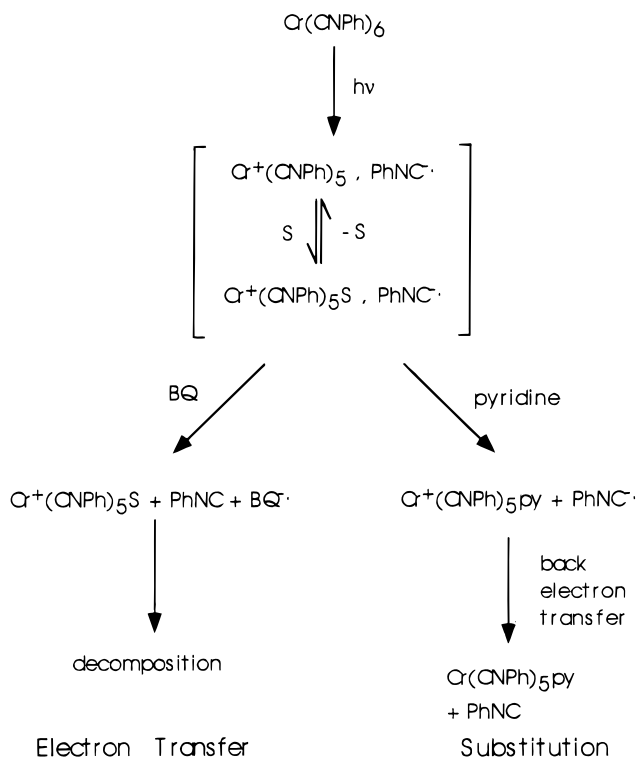
2. Electron Transfer Mediated Photosubstitution. We know that an excited state electron transfer cannot account for the concentration dependence of electron transfer described above. Therefore, electron transfer must occur from a reactive initial photoproduct. Quantum yield data suggests that substitution and electron transfer processes are linked: measured independently of each other, both processes have the same limiting quantum yield, 0.29, at 532 nm. To account for these observations, we suggest the pathway shown in Scheme 1. The dissociation of a phenylisocyanide radical anion directly and promptly from a MLCT state would give rise to the unusual combination of *both* substitution and electron transfer processes that are observed and provide an explanation for the concentration dependence of electron transfer. This model is consistent with the picosecond data that suggests that the formation of Cr(CNPh)₅S is 20 times less favorable at 532 nm than at 355 nm, even though substitution quantum yields are within a factor of 2 between these wavelengths (see Figure 1). With this model, the additional kinetic components of bleach recovery after 532 nm excitation can be assigned speculatively:



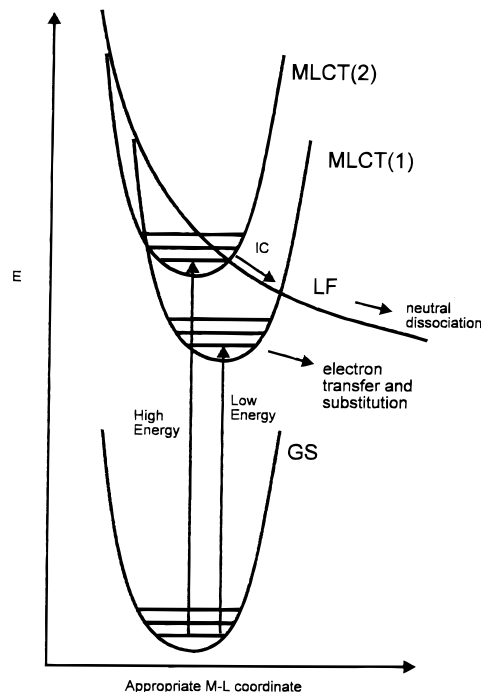
Cr⁺(CNPh)₅ and Cr⁺(CNPh)₅S may be formed initially in a nonequilibrium distribution. This is because the “naked” Cr⁺(CNPh)₅ fragment is expected to be initially highly vibrationally excited.

The excited state diagram in Scheme 2 provides a possible framework for the interpretation of the resonance Raman data

Scheme 1. Electron Transfer Mediated Photosubstitution Pathway in Cr(CNPh)₆



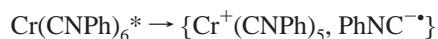
Scheme 2. Excited State Diagram of Cr(CNPh)₆



and the wavelength dependences of picosecond spectra, nanosecond kinetics, and the quantum yields for electron transfer and substitution. When Cr(CNPh)₆ is irradiated with a high-energy photon ($\approx 300\text{--}450$ nm), the higher MLCT(2) state is populated. An internal conversion (IC) to a ligand field state can occur, leading to charge-neutral dissociation of a PhNC ligand.

The MLCT(1) state is populated with low-energy photons ($\approx 450\text{--}550$ nm). This MLCT absorption is strongly coupled to the $\delta(\text{Cr}-\text{C}-\text{N})$ and $\delta(\text{C}-\text{Cr}-\text{C})$ bending vibrations (reso-

nance Raman data),⁴ providing distortions that may lead to substitution. The maximum yield for electron transfer occurs when this state is populated. The limiting yields for both substitution and electron transfer are the same in this region. We suggest that both reactions occur from the same primary process, namely, the formation of a radical pair:



From the wavelength dependence of electron transfer (Figure 3), it is clear that there is a wavelength region (≈ 360 – 480 nm) where the MLCT(1) pathway is present but does not account for 100% of the total substitution reactivity (Figure 1). There may be some overlap of MLCT absorptions that accounts for this behavior, or internal conversions between MLCT(1) and MLCT(2) are occurring, most likely from MLCT(2) to MLCT(1).

A previously reported wavelength dependence for photosubstitution in $\text{Cr}(\text{CNPh})_6$ had an unusual increase in ϕ_{sub} in the long-wavelength region.⁴ This was interpreted using the resonance Raman data above. That wavelength dependence was incorrect, probably due to errors in fulgide actinometry in the 400–450 nm region. In this work, the wavelength dependence for substitution in both benzene and pyridine (Figure 1) shows a simple decrease in ϕ_{sub} with decreasing energy across the wavelengths studied. The monotonic decreases are not interrupted with the change in substitution mechanism that occurs. The shape of the wavelength dependence of ϕ_{sub} seems to be independent of mechanism in $\text{Cr}(\text{CNPh})_6$.

The picosecond data on $\text{Cr}(\text{CNPh})_6$ indicate that primary products are formed in less than 20 ps at both 355 and 532 nm. Both reaction mechanisms involve primary photosteps that occur on the ultrafast time scale. The overall quantum yield is highly dependent on the excess excitation energy. If both reaction modes were occurring from thermally equilibrated excited states, ϕ_{sub} would change abruptly as the different states were populated. This is not the case here, and ϕ_{sub} seems more dependent on the caging dynamics of the system than on the nature of excited state populations.

An integral part of the coupled electron transfer–substitution mechanism proposed here is that $\text{PhNC}^{\bullet-}$ is responsible for electron transfer. An alternate possibility is that photoproduct $\text{Cr}(\text{CNPh})_5\text{S}$ is oxidized by benzoquinone. If that were the case, the quantum yields for electron transfer would be as high as the substitution yields at every wavelength studied. This is not the case.

The role of indirectly populated antibonding LF states in ultrafast photosubstitution reactions is a topic of current interest. For example, the photodissociation of CO in $\text{Mn}_2(\text{CO})_{10}$ and $\text{MnCl}(\text{CO})_5$ has been studied theoretically.²² In both systems, the antibonding LF states responsible for CO dissociation are

at high enough energy at equilibrium ground state geometries that they are not directly populated by irradiation into the lowest energy states, which are $\sigma \rightarrow \sigma^*$ states (antibonding for the Mn–Mn and Mn–Cl bonds). Despite this, CO loss occurs on excitation into these low-energy absorptions. There is significant theoretical evidence²⁰ that there is a precipitous decrease in the energies of the LF states with small increases in the Mn–CO bond length. A strongly avoided crossing between the LF state and the lowest energy excited state leads to an essentially barrierless CO dissociation. $\text{Cr}(\text{CNPh})_6$ is similar to these manganese carbonyls: the LF states are expected to lie at much higher energies than the MLCT states. The presence of a charge neutral, prompt, heterolytic pathway strongly implies the involvement of antibonding LF states.

The $\text{Cr}(\text{CNPh})_6$ system may constitute the first case of a photodissociation of an organic ligand radical *anion* directly and promptly from the corresponding MLCT state. Photochemical homolytic dissociation of alkyl, halide, or metal complex fragment radicals in group 7 complexes containing α -diimine ligands is well-known.^{2,3,23,24} Such reactions are thought to arise from σ – π^* states, labilizing bonds on the axis orthogonal to the metal– α -diimine ligand plane. The mechanism presented here for the low-energy $\text{Cr}(\text{CNPh})_6$ photochemistry is complementary to σ – σ^* reactivity in the sense that the excitation is localized on the ligand that is to be dissociated rather than on a neighboring group. The microscopic reasons for the dissociation of $\text{PhNC}^{\bullet-}$ on MLCT excitation are not entirely clear at this time. However, resonance enhancement of the Raman bands corresponding to the $\delta(\text{C}–\text{Cr}–\text{C})$ and $\delta(\text{Cr}–\text{C}–\text{N})$ bending vibrations indicates that these molecular distortions are coupled to the MLCT transition in the long-wavelength region.⁴ These distortions may lead to the ultrafast dissociation of $\text{PhNC}^{\bullet-}$.

Acknowledgment. This work was supported by the Natural Sciences and Engineering Research Council. We are indebted to Prof. A. D. Kirk at the University of Victoria for his assistance with the nanosecond flash photolysis experiments. Prof. I. S. Butler and his group at McGill University are acknowledged for their warm hospitality during visits to Montreal. Dr. Duane Friesen gave many helpful suggestions during this work.

Supporting Information Available: Listings of extinction coefficients, nanosecond flash photolysis kinetics, EPR data, experimental information on quantum yield determinations, and curve fitting procedures. This material is available free of charge via the Internet at <http://pubs.acs.org>.

IC9905650

- (22) (a) Rosa, A.; Ricciardi, G.; Baerends, E. J.; Stufkens, D. J. *Inorg. Chem.* **1995**, *34*, 3425. (b) Rosa, A.; Ricciardi, G.; Baerends, E. J.; Stufkens, D. J. *Inorg. Chem.* **1996**, *35*, 2886. (c) Wilms, M. P.; Baerends, E. J.; Rosa, A.; Stufkens, D. J. *Inorg. Chem.* **1997**, *36*, 1541.
 (23) Morse, D. L.; Wrighton, M. S. *J. Am. Chem. Soc.* **1976**, *98*, 3951.
 (24) Stufkens, D. J. *Comments Inorg. Chem.* **1992**, *13*, 359.